Transient effects and delay time in the dynamics of resonant tunneling

Gastón García-Calderón
Instituto de Física, Universidad Nacional Autónoma de México Apartado Postal 20-364, 01000 México, Distrito Federal, Mexico

Alberto Rubio
Facultad de Ciencias, Universidad Autónoma de Baja California, Apartado Postal 1880, Ensenada, Baja California, Mexico

(Received 24 June 1996)

We consider an analytic solution of the time-dependent Schrödinger equation with the initial condition $\psi(x,0)=\exp(ikx)$ along $-\infty<x<0$ to investigate the time evolution for $x>0$ of the wave function in a double-barrier resonant structure at resonance. For typical parameters of the structure we find that the single-resonance approximation is valid from a few tenths of the corresponding lifetime onward. Very short times require the contribution of many far away resonances. The buildup time along the internal region takes a few lifetimes. At birth the transmitted wave front is blurred; however, for long times it becomes well defined and moves with classical velocity yielding a delay time $\tau\approx 2\hbar/\Gamma$ as in the stationary-phase treatment. [S1050-2947(97)04105-X]

PACS number(s): 03.65.−w, 73.40.Gk

I. INTRODUCTION

Most studies on the dynamics of resonant tunneling have used approaches based on the numerical solution of the Schrödinger equation with the initial condition of a Gaussian wave packet [1–6]. The typical example for the analysis of resonant tunneling corresponds to that of a classically allowed region between two classically forbidden ones, namely, the double-barrier resonant structure. This system is of interest not only because it can be fabricated nowadays and possesses potential technological applications [7–9], but also because it lends itself to the investigation of basic issues of the physics of resonant tunneling.

In this work we consider a recent analytic approach that allows a general treatment of the dynamics of the tunneling process [10]. This approach consists of the solution of the time-dependent Schrödinger equation for an arbitrary potential $V(x)$ defined in the region $0\leq x\leq L$ with the initial condition at $t=0$ of a plane wave of momentum k confined in the half space $x<0$ to the left of a shutter located at $x=0$. The sudden opening of the shutter at the time $t=0$ allows the wave to propagate into the region $x>0$. It may be shown that as the time t goes to infinity, the wave solution tends to the stationary solution of the Schrödinger equation [10]. In this sense this approach is complementary to those based on finite-width wave packets that do not permit one to analyze the transition to the stationary case. The shutter problem for the time propagation of a free wave was initially considered by Moshinsky [11]. He found that both the current and the probability density for a fixed value of the time t as a function of the distance x, or for a fixed value of x as a function of t, present oscillations near the wave front, a phenomenon he named diffraction in time [11]. More recently, the shutter problem has been extended to the case of a δ potential by Eberfeld and Kleber [12,13] and considered also by other authors [14]. An experimental observation of diffraction in time has been recently reported by Szriftgiser *et al.* [15].

The purpose of this work is to apply the approach developed in Ref. [10] to investigate the time evolution of a plane wave whose energy coincides with the resonance energy of a double-barrier resonant structure (Fig. 1). Specifically, we are interested in the analysis of the buildup process that leads to the stationary-wave solution both for the internal region of the potential and for the transmitted propagating-wave solution along the region $x>L$. We also investigate the wave front of the transmitted wave for large times, i.e., much longer than the time scale given by the lifetime of the resonance, and compare it with the free propagating case to study the notion of delay time from a dynamical point of view.

The work is organized as follows. In Sec. II we present a derivation of the formalism. Section III deals with some numerical examples for both the internal and external regions of the potential. In Sec. IV we discuss the notion of delay time from a dynamical point of view. Finally, Sec. V contains the conclusions.

II. FORMALISM

For the sake of completeness we present here a more detailed derivation of the solution $\psi(x,t)$ of the time-dependent Schrödinger equation for $x>0$ and $t>0$ given by García-Calderón [10]. Let us consider the time-dependent Schrödinger equation

$$i\hbar\left(\frac{\partial}{\partial t}-H\right)\psi(x,t)=0, \qquad (2.1)$$

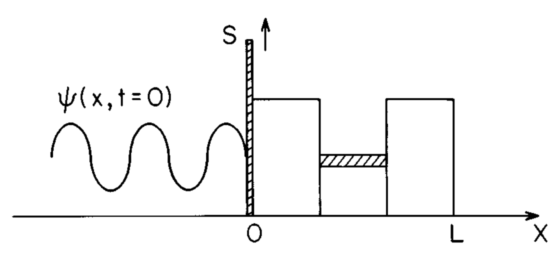

FIG. 1. Shutter problem for a double-barrier resonant structure. A plane wave in the region $x<0$ is instantaneously released at $t=0$ by the removal of shutter S.

where $H=-(\hbar^2/2m)d^2/dx^2+V(x)$ and $V(x)$ describes a resonant tunneling potential profile of arbitrary shape extending from $x=0$ to $x=L$. The initial value $\psi(x,t=0)$ is chosen to be

$$\psi(x,t=0)=\begin{cases} e^{ikx}, & x<0 \\ 0, & x>L. \end{cases} \tag{2.2}$$

Note that e^{ikx} extends only through a half space, so it cannot be normalized in the usual way. One may Laplace transform Eq. (2.1) using the standard definition

$$\overline{\psi}(x,k,s)=\int_0^\infty \psi(x,k,t)e^{-st}dt, \tag{2.3}$$

with the initial condition (2.2). It is convenient to make the change of variable $s=-ip^2/\alpha$ with $\alpha=2m/\hbar$ to write the Laplace-transformed equations

$$\left(\frac{\partial^2}{\partial x^2}+p^2\right)\overline{\psi}(x,p)=i\alpha e^{ikx}, \quad x\leqslant 0, \tag{2.4}$$

where the inhomogeneous term arises from the initial condition (2.2),

$$\left(\frac{\partial^2}{\partial x^2}+p^2-V(x)\right)\overline{\psi}(x,p)=0, \quad 0\leqslant x\leqslant L, \tag{2.5}$$

and

$$\left(\frac{\partial^2}{\partial x^2}+p^2\right)\overline{\psi}(x,p)=0, \quad x\geqslant L. \tag{2.6}$$

The Laplace-transformed solutions for Eqs. (2.4) and (2.6) are given, respectively, as

$$\overline{\psi}(x,p)=\begin{cases} i\alpha(p^2-k^2)^{-1}e^{ikx}+C(p)e^{-ipx}, & x\leqslant 0 \quad (2.7)\\ D(p)e^{ipx}, & x\geqslant L. \quad (2.8)\end{cases}$$

In Eq. (2.7) the first term on the right-hand side corresponds to a particular solution of the inhomogeneous equation (2.4). Notice that the solutions $C(p)\exp(-ipx)$ and $D(p)\exp(ipx)$ appearing, respectively, in Eqs. (2.7) and (2.8) are the only physically acceptable solutions to Eqs. (2.4) and (2.6) since $p=\alpha(1+i)(s/2)^{1/2}$.

Along the internal region of the potential it is convenient to write the solution $\overline{\psi}(x,p)$ in terms of the outgoing Green's function $G^+(x,x';p)$ that satisfies the equation

$$\left(\frac{\partial^2}{\partial x^2}+p^2-V(x)\right)G^+(x,x';p)=\delta(x-x'), \quad 0\leqslant x\leqslant L, \tag{2.9}$$

with the outgoing boundary conditions

$$\left[\frac{\partial}{\partial x}G^+(x,x';p)\right]_{x=0_-}=-ipG^+(0,x';p) \tag{2.10}$$

and

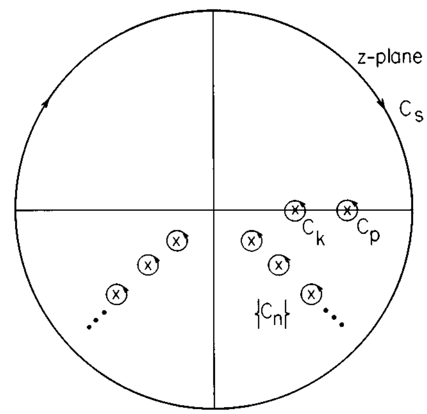

FIG. 2. Integration contour $\Gamma=\Sigma_n c_n+c_p+c_k+c_s$ used to evaluate Eqs. (2.15) and (2.33).

$$\left[\frac{\partial}{\partial x}G^+(x,x';p)\right]_{x=L_+}=ipG^+(L,x';p). \tag{2.11}$$

Let us multiply Eq. (2.9) by $\overline{\psi}(x,p)$ and subtract from it Eq. (2.5) multiplied by $G^+(x,x';p)$ followed by integration along the region from $x=0$ to $x=L$. Using Eqs. (2.7), (2.10), and (2.11) yields an expression that relates $\overline{\psi}(x,p)$ with the outgoing propagator

$$\overline{\psi}(x,p)=\frac{\alpha}{k-p}G^+(0,x;p) \quad (0\leqslant x\leqslant L). \tag{2.12}$$

Evaluating Eqs. (2.8) and (2.12) at $x=L$ allows us to write the coefficient $D(p)$ as

$$D(p)=\frac{\alpha}{k-p}G^+(0,L;p)e^{-ipL}. \tag{2.13}$$

Hence for $x>L$, $\overline{\psi}(x,p)$ may be written as

$$\overline{\psi}(x,p)=\frac{\alpha}{k-p}G^+(0,L;p)e^{-ipL}e^{ipx} \quad (x>L). \tag{2.14}$$

Equations (2.12) and (2.14) are very convenient because one can exploit the analytical properties of the propagator on the complex p plane to obtain appropriate expressions from which the corresponding inverse Laplace transform can be evaluated.

A. Internal region

Let us consider the analytical continuation of the solution $\overline{\psi}(x,p)$, defined along the internal region $0\leqslant x\leqslant L$, over the complex p plane. Take $p\rightarrow z$ and write the Cauchy contour integral

$$\frac{1}{2\pi i}\oint_\Gamma \frac{z\overline{\psi}(x,z)}{z-p}dz=0, \tag{2.15}$$

where the contour Γ is as shown in Fig. 2 and is formed by the sum of small circles $\{c_n\}$, associated with the complex poles $k_n=a_n-ib_n$ of the propagator, and c_p and c_k, surrounding, respectively, poles at $z=p$ and $z=k$, all enclosed by the large circle c_s, i.e., $\Gamma=\Sigma_n c_n+c_p+c_k+c_s$. It can be shown along the same lines as Ref. [16] that for $0<x\leq L$, the integral over c_s vanishes as its radius tends to infinity. Consequently, Eq. (2.15) can be written as

$$\frac{1}{2\pi i}\left\{\oint_{c_p}\frac{z\overline{\psi}(x,z)}{z-p}dz-\oint_{c_k}\frac{\alpha zG^{+}(0,x;z)}{(z-p)(z-k)}dz -\sum_n\oint_{c_n}\frac{\alpha zG^{+}(0,x;z)}{(z-p)(z-k)}dz\right\}=0. \tag{2.16}$$

Next we apply the theorem of residues to evaluate the integrals above. The residue of the propagator $G^{+}(x,x';k)$ at each pole $k_n=a_n-ib_n$, with $(a_n,b_n)>0$, can be written in terms of the function $u_n(x)$ obeying the Schrödinger equation of the problem with outgoing boundary conditions, as shown in Appendix A, namely,

$$\text{res}G^{+}(x,x';k)=\frac{u_n(x)u_n(x')}{2k_n}. \tag{2.17}$$

Hence Eq. (2.16) may be written as

$$p\overline{\psi}(x,k,p)=\alpha\frac{kG^{+}(0,x;k)}{(k-p)}+\alpha\sum_n\frac{u_n(0)u_n(x)}{2(p-k_n)(k-k_n)}. \tag{2.18}$$

The inverse Laplace transform is given by

$$\psi(x,k,t)=\frac{1}{2\pi i}\int_{c-i\infty}^{c+i\infty}\overline{\psi}(x,k,p)e^{-ip^2t/\alpha}\left(\frac{-2i}{\alpha}\right)p\ dp. \tag{2.19}$$

Substitution of Eq. (2.18) into Eq. (2.19) yields

$$\psi(x,k,t)=\phi(x,k)M(0,k,t)-i\sum_n\frac{u_n(0)u_n(x)}{k-k_n}M(0,k_n,t)\qquad(0<x\leq L), \tag{2.20}$$

where $\phi(x,k)=2ikG^{+}(0,x;k)$ stands for the stationary solution to the Schrödinger equation [17] and the index n runs over all the poles, which are located on the third and fourth quadrants of the complex k plane. The poles on the third quadrant denoted by k_{-r} are related to those on the fourth k_r, by $k_{-r}=-k_r^*$ (r positive). In what follows k_n stands for any pole unless explicitly indicated by the subindex r. The Moshinsky functions $M(0,k,t)$ and $M(0,k_n,t)$ in Eq. (2.20) are defined as [18,19,11]

$$M(0,q,t)=\frac{i}{2\pi}\int_{-\infty}^{\infty}\frac{e^{-ip^2t/\alpha}}{p-q}\ dp=\frac{1}{2}e^{y^2}\text{erfc}(y), \tag{2.21}$$

where $q=k,k_n$ and the argument y is given by

$$y\equiv-e^{-i\pi/4}\left(\frac{m}{2\hbar}\right)^{1/2}\left[\frac{\hbar q}{m}t^{1/2}\right]. \tag{2.22}$$

Equation (2.20) gives an exact expression for the time evolution of the wave function $\psi(x,t)$ along the internal region of the double-barrier system. Notice that the derivation is not based on a particular potential profile and therefore, as pointed out in Ref. [10], the above equation is valid for an arbitrary potential provided it vanishes after a distance. Note also that the expansion (2.20) does not apply at $x=0$ where subtractions are required to ensure convergence [16].

It is of interest to direct the attention of the reader to the limits of Eq. (2.20) for $\psi(x,t)$, as the time $t\to 0$ and also when t becomes very large. At $t=0$ the solution $\psi(x,k,t)$ must vanish for $x>0$ as specified by the initial condition (2.2). It follows from Eq. (B4) that for $t=0$, the Moshinsky functions appearing in Eq. (2.20) attain the value

$$M(0,k,t=0)=M(0,k_n,t=0)=\frac{1}{2}, \tag{2.23}$$

with q_n either k_r or k_{-r} as specified above, and hence Eq. (2.20) becomes

$$\psi(x,k,t=0)=\frac{1}{2}\phi(x,k)-\frac{1}{2}i\sum_n\frac{u_n(0)u_n(x)}{k-k_n}\qquad(0<x\leq L). \tag{2.24}$$

Since the stationary solution $\phi(x,k)$ admits the resonant expansion [16]

$$\phi(x,k)=ik\sum_n\frac{u_n(0)u_n(x)}{k_n(k-k_n)}\qquad(0<x\leq L) \tag{2.25}$$

and furthermore resonant states fulfill [16]

$$\sum_n\frac{u_n(0)u_n(x)}{k_n}=0\qquad(0<x\leq L), \tag{2.26}$$

it follows, using the identity

$$\frac{k}{k_n(k-k_n)}\equiv\frac{1}{k_n}+\frac{1}{k-k_n}, \tag{2.27}$$

that Eq. (2.24) vanishes exactly. It is interesting to note that in a single-term approximation, $\psi(x,k,t=0)$ is given by

$$\psi(x,k,t=0)=\frac{1}{2}i\frac{u_n(0)u_n(x)}{k_n}\qquad(0<x\leq L), \tag{2.28}$$

which might be very small, but strictly differs from zero. It is also worth noticing that the very-short-time behavior of $\psi(x,k,t)$ may involve the contribution of far away resonance terms.

The long-time limit of $\psi(x,k,t)$ [see Eq. (2.20)] is given by the asymptotic behavior of the Moshinsky functions $M(0,q,t)$. For $q=k$ it follows from Eq. (2.22) that $\arg y=3\pi/4$ and hence from Eq. (B9), $M(0,k,t)$ behaves as

$$M(0,k,t)\to e^{-iEt/\hbar},\qquad t\to\infty, \tag{2.29}$$

namely, $M(0,k,t)$ goes into the time dependence of the stationary solution of the Schrödinger equation. For the long-time limit of the functions $M(0,k_n,t)$ appearing in Eq. (2.21), one has to distinguish the cases $q=k_{-r}$ and $q=k_r$. For $q=k_{-r}\equiv-k_r^*$, denoting the corresponding M function as $M(0,k_{-r},t)$, it follows from Eq. (2.22) that $-\pi/2<\arg y<\pi/2$ and hence from Eq. (B6) (with $x=0$) one obtains at long times

$$M(0,k_{-r},t)\approx\frac{a}{t^{1/2}}+\frac{b}{t^{3/2}}+\cdots, \tag{2.30}$$

where a and b are independent of time. Evidently, Eq. (2.30) vanishes as $t\to\infty$. For $q=k_r$, denoting the M function as $M(0,k_r,t)$, it now follows from Eq. (2.22) that $\pi/2<\arg y<3\pi/2$, and consequently from Eq. (B9) (with $x=0$) one gets at very long times

$$M(0,k_r,t)\approx e^{-iE_rt/\hbar}+\frac{a}{t^{1/2}}+\frac{b}{t^{3/2}}+\cdots, \tag{2.31}$$

where the first term on the right-hand side exhibits exponential decay with time since $E_r=\epsilon_r-i\Gamma_r/2$. Again, Eq. (2.31) vanishes as $t\to\infty$. The functions $M(0,k_{-r},t)$ and $M(0,k_r,t)$ are also relevant in studies on the nonexponential contributions to decay [20]. Hence it follows from the above analysis that at very long times $\psi(x,k,t)$ goes into the stationary solution

$$\psi(x,k,t)=\phi(x,k)e^{-iEt/\hbar}\quad (0<x\leq L). \tag{2.32}$$

B. External region

The analysis of the external region $x>L$ proceeds essentially along similar lines to that of the preceding subsection. Here it is convenient to consider a contour integral for the coefficient $D(p)$ as defined by Eq. (2.13). Hence, instead of Eq. (2.15) we evaluate

$$\frac{1}{2\pi i}\oint_\Gamma \frac{zD(z,k)}{z-p}dz=0. \tag{2.33}$$

After a few manipulations we obtain

$$pD(p,k)=\alpha\frac{kG^+(0,L;k)}{(k-p)}+\alpha\sum_n \frac{u_n(0)u_n(x)e^{-ik_nL}}{2(p-k_n)(k-k_n)}. \tag{2.34}$$

Substitution of Eq. (2.34) into Eq. (2.8) and the result into the inverse Laplace transform (2.19) yields

$$\psi(x,k,t)=T(k)M(x,k,t)-i\sum_n \frac{u_n(0)u_n(L)e^{-ik_nL}}{(k-k_n)}M(x,k_n,t)\quad (x\geq L), \tag{2.35}$$

where $T(k)=2ikG^+(0,L,k)e^{-ikL}$ stands for the transmission amplitude of the problem [17] and the Moshinsky functions $M(x,q,t)$, with $q=k,k_n$, are now defined as [18,19,11]

$$M(x,q,t)=\frac{i}{2\pi}\int_{-\infty}^{\infty}\frac{e^{ipx}e^{-ip^2t/\alpha}}{p-q}\,dp=\frac{1}{2}e^{imx^2/2\hbar t}e^{y^2}\mathrm{erfc}(y) \tag{2.36}$$

where the argument y is, in this case, given by

$$y\equiv e^{-i\pi/4}\left(\frac{m}{2\hbar t}\right)^{1/2}\left[x-\frac{\hbar q}{m}t\right]. \tag{2.37}$$

Equation (2.35) provides an exact expression for the time evolution of the wave function along the transmitted region $x\geq L$. As in Sec. II A, it is of interest to analyze the limits of $\psi(x,k,t)$ both as the time goes to zero and as it becomes very large. It turns out that in both limits Eq. (2.37) becomes very large. Indeed, it follows from Eq. (2.37) that a very short time implies a very large argument y, i.e.,

$$y\approx e^{-i\pi/4}\left(\frac{m}{2\hbar t}\right)^{1/2}x, \tag{2.38}$$

which is independent of the value of q. Consequently, using Eq. (B6),

$$M(x,q,t)\approx e^{i\pi/4}\left(\frac{2\hbar}{mx^2}\right)^{1/2}t^{1/2} \tag{2.39}$$

and hence $M(x,k,t)$, $M(x,k_{-r},t)$, and $M(x,k_r,t)$ vanish as $t\to 0$. Therefore, $\psi(x,k,t=0)$ vanishes as expected from the initial condition. For very large times, the argument y in Eq. (2.37) becomes also very large, namely,

$$y\approx -e^{-i\pi/4}\left(\frac{m}{2\hbar}\right)^{1/2}\left[\frac{\hbar q}{m}t^{1/2}\right]. \tag{2.40}$$

The above expression depends on the choice of q. For $q=k$, it follows from Eq. (2.40) that $\arg y=3\pi/4$ and hence from Eq. (B9) $M(x,k,t)$ tends to the stationary form of the wave function as $t\to\infty$,

$$M(x,k,t)\to e^{ikx}e^{-iEt/\hbar}\quad (t\to\infty). \tag{2.41}$$

The functions $M(x,k_r,t)$ and $M(x,k_{-r},t)$ behave at long times in a similar fashion to the functions $M(0,k_r,t)$ and $M(0,k_{-r},t)$ discussed in Sec. II B. Indeed, for $q=k_{-r}=-k_r^*$, it is easily seen from Eq. (2.40) that $-\pi/2<\arg y<\pi/2$ and hence $M(x,k_{-r},t)$ behaves as Eq. (B6) and, as $t\to\infty$, it vanishes. Finally, for $q=k_r$ it follows from Eq. (2.40) that $\pi/2<\arg y<3\pi/2$ and hence from Eq. (B9) $M(x,k_r,t)$ vanishes also as $t\to\infty$ since $\exp(-iE_rt)$ decays exponentially with time. Therefore, at very long times the solution $\psi(x,k,t)$ along the external region, given by Eq. (2.35), tends to the stationary form of the wave function

$$\psi(x,k,t)=T(k)e^{ikx}e^{-iEt/\hbar}\quad (x\geq L). \tag{2.42}$$

C. Remarks

The solution $\psi(x,k,t)$ of the shutter problem for the potential $V(x)$ as given by Eqs. (2.20) and (2.35) represents an expansion in terms of resonant states and M functions. Notice that in the absence of an interaction $V(x)$, there are no complex poles. The solution (2.20) does not exist, since there is no internal region, and the solution (2.35) goes into the free solution obtained by Moshinsky [11]

$$\psi(x,k,t)=M(x,k,t)\quad (x>0). \tag{2.43}$$

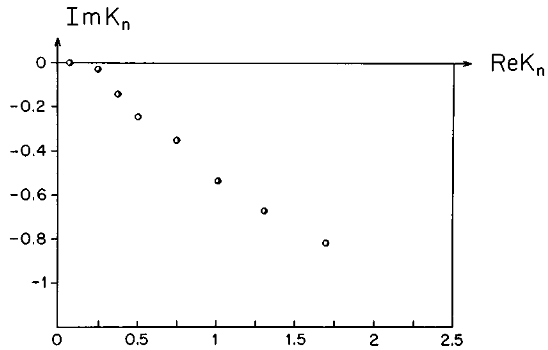

FIG. 3. First eight complex poles of the outgoing Green's function on the E plane corresponding to the double-barrier structure depicted in Fig. 1 with the parameters $V_0=0.23$ eV and $b=w=50$ Å.

As soon as the time $t\neq 0$, each term in Eqs. (2.20) and (2.35) contributes to yield a finite, yet very small, probability to find the particle along the full region $x>0$. This is also the case for the free case given by Eq. (2.43). The above situation exhibits a nonlocal feature of the time-dependent solution [10] and it results from the fact that in a nonrelativistic description, there is no restriction on the velocity of some components of the initially confined wave function to the region $x<0$. It might be of interest to mention that in fully relativistic quantum field theories it has been pointed out by Hegerfeldt [21] that the sudden opening of a shutter at $t=0$ may also lead to the same sort of nonlocal effects. This leads to a causality problem since it implies a violation of Einstein causality, i.e., no propagation faster than light. Hegerfeldt argues that the above difficulty is of a theoretical nature and discusses a number of ways out. However, in our nonrelativistic approach the violation of Einstein causality should not be surprising.

The example presented in the next section shows the buildup of the probability density along the internal region and the birth and formation of the propagating probability density along the external region. As we shall see, at a given time, the nonlocal aspects of the propagating solution are exhibited as an exceedingly small precursor extending at any distance beyond the wave front.

III. EXAMPLE

In this section we consider the example of a double-barrier resonant structure with typical parameters [7,8] to investigate the time evolution of $\psi(x,k,t)$ along both the internal and external regions of the potential. We choose the following parameters for the system: barrier heights $V_0=0.23$ eV, barrier and well widths $bw=50$ Å, and effective mass for the electron $m=0.067m_e$. The resonance parameters $\{E_n\}$, with $E_n=\epsilon_n-i\Gamma_n/2=\hbar^2k_n^2/2m$, and the corresponding resonant eigenfunctions $\{u_n(x)\}$ can be obtained by a straightforward calculation using the transfer matrix method adapted to outgoing boundary conditions [22]. The first few poles are shown in Fig. 3. We find in our calculations that for times roughly of the order of 0.1τ onward, the single-resonance term approximation to the expansions (2.20) and (2.35) for $\psi(x,k,t)$ is quite good. However, for shorter times, both for the internal and external regions, one has to take into account the contribution of additional resonance terms. In this regime the probability density is quite small and it might be beyond experimental observation. A detailed analysis of this regime of very early times will be considered elsewhere [23]. For energies near the resonance energy E_1 one may write the single resonance approximations to Eqs. (2.20) and (2.35), namely,

$$\psi(x,k,t)\approx i\frac{u_1(0)u_1(x)}{k-k_1}\left[\frac{k}{k_1}M(0,k,t)-M(0,k_1,t)\right] \quad (0<x\leqslant L) \quad (3.1)$$

and

$$\psi(x,k,t)\approx i\frac{u_1(0)u_1(L)}{k-k_1}\left[\frac{k}{k_1}M(x,k,t)e^{-ikL} - M(x,k_1,t)e^{-ik_1L}\right] \quad (x\geqslant L). \quad (3.2)$$

At long times one may use Eqs. (2.32) and (2.42) to write Eqs. (3.1) and (2.35), respectively, as

$$\psi(x,k,t)\approx i\frac{u_1(0)u_1(x)}{k-k_1}\left[\frac{k}{k_1}e^{-iEt/\hbar}\right] \quad (0<x\leqslant L) \quad (3.3)$$

and

$$\psi(x,k,t)\approx i\frac{u_1(0)u_1(L)}{k-k_1}\left[\frac{k}{k_1}e^{-ikL}e^{ikx}e^{-iEt/\hbar}\right] \quad (x\geqslant L). \quad (3.4)$$

Note that $u_1(0)$ and $u_1(L)$ are proportional to the partial decay widths of the corresponding resonance state [22]. It is appealing to write the probability densities to Eqs. (3.3) and (3.4) in the energy plane in a Breit-Wigner fashion, namely,

$$|\psi(x,k,t)|^2\approx\frac{\Gamma_1^0}{(E-\epsilon_1)^2+\Gamma_1^2/4}|u_1(x)|^2 \quad (0<x\leqslant L) \quad (3.5)$$

and

$$|\psi(x,k,t)|^2\approx\frac{\Gamma_1^0\Gamma_1^L}{(E-\epsilon_1)^2+\Gamma_1^2/4} \quad (x\geqslant L). \quad (3.6)$$

Equations (3.5) and (3.6) hold far from threshold, namely, for an isolated sharp resonance. The decay width $\Gamma_1=\Gamma_1^0+\Gamma_1^L$ and the partial decay widths Γ_1^0 and Γ_1^L are defined as [22]

$$\Gamma_1^0=\frac{\hbar a_1}{m}\frac{|u_1(0)|^2}{I_1}, \quad \Gamma_1^L=\frac{\hbar a_1}{m}\frac{|u_1(L)|^2}{I_1}. \quad (3.7)$$

In Eqs. (3.7) $a_1=\mathrm{Re}k_1$ and I_1 is a quantity of the order of unity [22]. For a symmetrical structure $\Gamma_1^0=\Gamma_1^L=\Gamma_1/2$ and hence, for example, at resonance energy $E=\epsilon_1$, Eq. (3.6) becomes unity. The resonance parameters of the problem for lowest resonance $n=1$ are $\epsilon_1=0.080\,054$ eV and

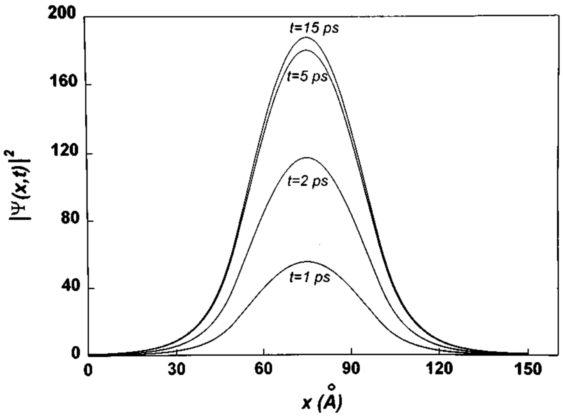

FIG. 4. Plot of $|\psi(x,k,t)|^2$ for times $t=$ 1,2,5,15 ps, showing the buildup along the internal region.

$\Gamma_1=0.001\,028$ eV. The lifetime $\tau=\hbar/\Gamma_1$ associated with this resonance state is $\tau=0.64$ ps.

A. Results for the internal region

We have evaluated Eq. (3.1) for $\psi(x,k,t)$ to plot the probability density $|\psi(x,k,t)|^2$ along the internal region from $x=0$ to $x=L=150$ Å, with $k=(2m\epsilon_1)^{1/2}/\hbar$, as shown in Fig. 4. The figure exhibits the building up of the probability density for times 1, 2, 5, and 15 ps, showing the transient behavior towards the stationary value. In our example this occurs around a time $t_0\approx 10$ ps, as is made evident in Fig. 5, which shows the probability density evaluated at the fixed value of $x=75$ Å, where the probability acquires its maximum value, as a function of time. This figure also displays the contribution of the decaying term, i.e., the second term on the right-hand side of the probability density (3.1).

B. Results for the external region

For the external region one sees from Eq. (3.2) that as soon as the time t differs from zero $t\neq 0$, the transmitted probability density acquires a value different from zero over the whole space region $x\geqslant L$. Figure 6 shows the birth of the transmitted probability function and how it evolves with time

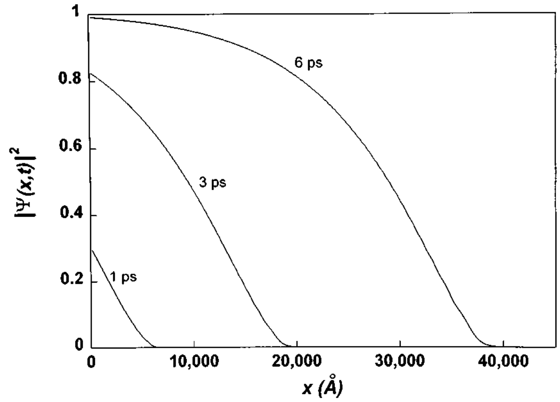

FIG. 6. Plot of $|\psi(x,k,t)|^2$ as a function of the distance x for three times $t=1,3,6$ ps. This graph shows the birth and growth of the transmitted wave. Note that the lifetime of the resonance is $\tau=0.64$ ps.

from 1 to 6 ps. In Fig. 7 we show the subsequent time evolution for $|\psi(x,k,t)|^2$ for three values of the time from 15 to 100 ps. As can be seen, the wave front becomes well defined, turning sharper, as time goes on. The wave front advances with the classical velocity $v=\hbar k/m$. As in the case for the internal region, the very-short-time regime corresponds to a very small probability density and requires also one to take into account additional resonance terms. The propagation can also be seen in Fig. 8, which shows $|\psi(x,k,t)|^2$ as a function of time for two fixed positions. This case is analogous to Fig. 5 for the internal region. The stationary value is also reached around 10 ps. In all the cases studied, as soon as $t\neq 0$, the solution is different from zero along the whole space $x>L\perp$. Nevertheless, we find that the value of the probability density is exceedingly small beyond the propagating wave front. In order to illustrate this situation we plot in Fig. 9 $|\psi(x,t)|^2$ for $t=6$ ps for values of x between 90 000 Å and 100 000 Å. The wave front corresponding to this case, situated near 40 000 Å, is shown in Fig. 6. It follows from Eq. (2.39) that for a fixed value of the time, the precursor strictly vanishes only in the limit $x\rightarrow\infty$. The small observed oscillatory behavior in Fig. 9 is washed out by adding more resonance terms to the calculation.

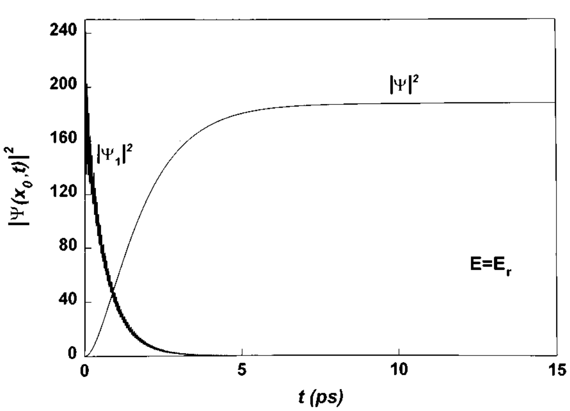

FIG. 5. Plot of $|\psi(x,k,t)|^2$ for a fixed value $x=75$ Å as a function of time to exhibit the transient behavior of the solution and the onset to the stationary solution at long times. Also shown is the decaying contribution $|\psi_1(x,k,t)|^2$ to the probability density

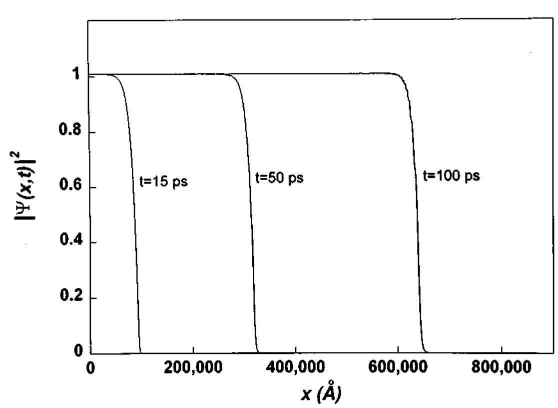

FIG. 7. This graph, as the previous one, shows the evolution of $|\psi(x,k,t)|^2$, now for longer times $t=$ 15,50,100 ps. Note, by comparison with the previous graph, that the wave front becomes sharper as time increases.

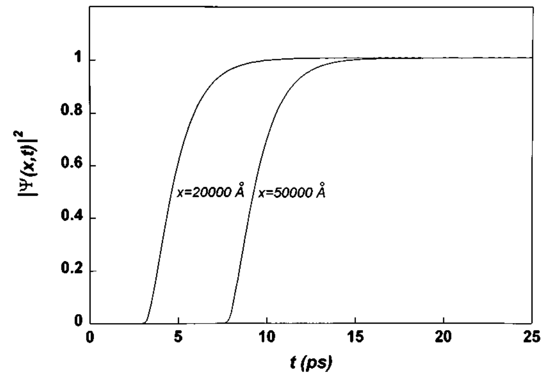

FIG. 8. Plot of $|\psi(x,k,t)|^2$ for two values of x as a function of time to show the transient behavior leading to the stationary value in the external region as time increases.

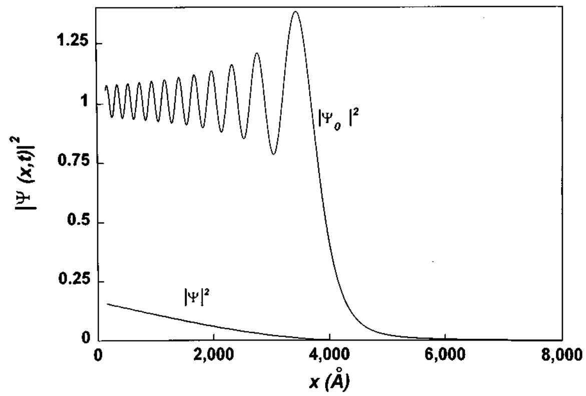

FIG. 10. Comparison of the free-wave time evolution $|\psi_0(x,k,t)|^2$ with the solution transmitted across the system $|\psi(x,k,t)|^2$ for a short time of the order of the lifetime $\tau = 0.64$ ps. Since the transmitted wave front is not yet sharp enough, it is not possible to measure the delay confidently.

IV. DELAY TIME

The notion of delay time arises from a stationary-phase argument for the transmitted wave packet [24,25]. It is well known that the delay time may be expressed in terms of the energy derivative of the phase of the transmission amplitude, namely,

$$\tau_\theta = \hbar \frac{d\theta}{dE}. \tag{4.1}$$

Near resonance energy the following analytic expression for the delay time may be obtained [26]:

$$\tau_\theta \approx \hbar \frac{\Gamma_1/2}{(E-\epsilon_1)^2 + \Gamma_1^2/4}. \tag{4.2}$$

Clearly at resonance energy $E = \epsilon_1$, $\tau_\theta \approx 2\hbar/\Gamma_1$.

We have compared the transmitted probability density $|\psi(x,k,t)|^2$ across the double-barrier resonant structure with the free-wave probability density for two cases: one, given in Fig. 10, for a short time of the order of one lifetime, i.e., $t = 0.64$ ps, and the other case for a much longer time $t = 1540$ ps, corresponding to a wave front at $x \approx 0.1$ cm, given in Fig. 11. In both cases one observes a delay time of the transmitted case relative to the free situation. In Fig. 10 the transmitted probability density is blurred and it does not allow one to estimate confidently the delay time. On the other hand, in Fig. 11, where the transmitted wave front is sharper, the delay can be estimated to be roughly of the order of $2\hbar/\Gamma_1$, which agrees with the stationary-phase value at resonance energy. The above considerations imply that the notion of delay time is an asymptotic property and provide also a measurement of the delay time using a dynamical analysis of the wave-packet propagation. This result deserves further analysis.

V. CONCLUDING REMARKS

An important feature of our approach is that it allows us to observe clearly the transient effects associated with the time evolution of a wave solution at resonance energy across and beyond a resonant tunneling structure. It is found, for typical parameters of the system, that the transient is of the order of a few lifetimes. Along the internal region of the potential the transient consists of the building up of the reso-

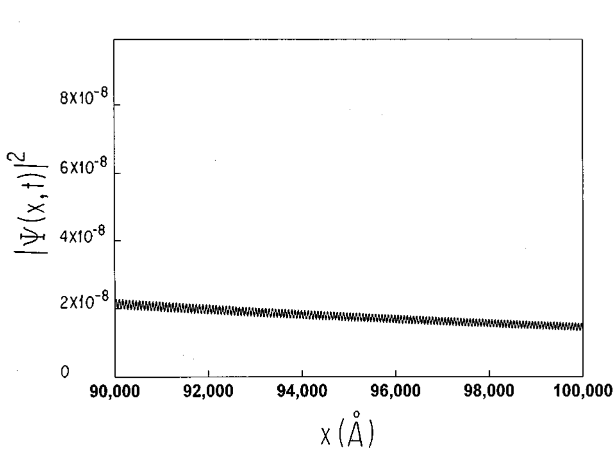

FIG. 9. Plot of $|\psi(x,k,t)|^2$ at $t=$ 6 ps for x from 90 000 Å up to 100 000 Å. This graph shows the nonvanishing, though exceedingly small, precursor beyond the wave front. The wave front corresponding to this case occurs near 40 000 Å as shown in Fig. 6.

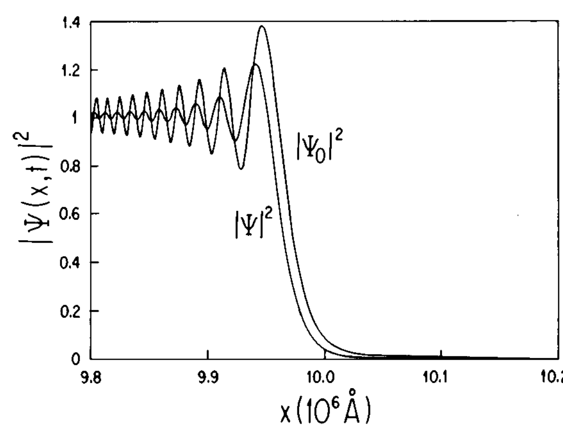

FIG. 11. Comparison of the free-wave time evolution $|\psi_0(x,k,t)|^2$ with the solution transmitted across the system $|\psi(x,k,t)|^2$ for a longer time $t=$ 1540 ps (corresponding to a wave front at $x \approx 0.1$ cm) to show that the delay time is of the order of $2\hbar/\Gamma_1$.

nant solution until the stationary solution is reached. Along the external region, one observes the birth of the propagating wave front and after a few lifetimes the transmitted wave front propagates virtually with the classical velocity $v=\hbar k/m$. Our approach provides a dynamical analysis of the delay time that the transmitted wave solution suffers with respect to the free propagating wave. We found a delay time of the order of $2\hbar/\Gamma_1$, as obtained using a stationary-phase argument. Our analysis shows also the absence of propagation along the internal region, at least for times longer than a fraction of a lifetime. Our work exhibits a nonlocal character of the quantum-mechanical propagation. This appears as an exceedingly small precursor covering the whole space as soon as the time differs from zero. Along the internal region of the interaction one observes how this precursor builds up as time evolves until the stationary solution is reached, whereas along the external region, it remains negligibly small at distances beyond the propagating wave front. It is worth stressing that for times longer than one-tenth of a lifetime onward the single-term approximation to our expansions is quite accurate.

ACKNOWLEDGMENTS

Tha authors acknowledge financial support from ConacyT, Mexico through Contract No. 2028-9302. G.G.C. would like to thank Marcos Moshinsky for useful discussions on the shutter problem. He has also benefited from discussions with colleagues Ana María Cetto, Luis de la Peña, and José Luis Mateos.

APPENDIX A: DETERMINATION OF THE RESIDUE AT A POLE OF THE GREEN FUNCTION

In what follows it is shown that the residue of $G^+(x,x';k)$ near one of its complex poles is proportional to the functions $u_n(x)$ and $u_n(x')$. In doing so we apply to one dimension the derivation of García-Calderón and Peierls [27]. This is of interest because the normalization condition for resonant states in one dimension differs from that in three dimensions.

The resonant function $u_n(x)$ for a Hamiltonian $H=T+V$, with $V(x)$ extending from $x=0$ to $x=L$, obeys the Schrödinger equation

$$\frac{d^2}{dx^2}u_n(x)+[k_n^2-V(x)]u_n(x)=0 \qquad \text{(A1)}$$

and satisfies the boundary conditions at $x=0$ and $x=L$,

$$\left[\frac{d}{dx}u_n(x)\right]_{x=0_-}=-ik_nu_n(0) \qquad \text{(A2)}$$

and

$$\left[\frac{d}{dx}u_n(x)\right]_{x=L_-}=ik_nu_n(L). \qquad \text{(A3)}$$

On the other hand, the outgoing Green's function associated with the Hamiltonian H satisfies the equation

$$\frac{\partial^2}{\partial x^2}G^+(x,x';k)+[k^2-V(x)]G^+(x,x';k)=\delta(x-x'), \qquad \text{(A4)}$$

with the boundary conditions at $x=0$ and $x=L$ given, respectively, by

$$\left[\frac{\partial}{\partial x}G^+(x,x';k)\right]_{x=0_-}=-ikG^+(0,x';k) \qquad \text{(A5)}$$

and

$$\left[\frac{\partial}{\partial x}G^+(x,x';k)\right]_{x=L_-}=ikG^+(L,x';k). \qquad \text{(A6)}$$

Near a complex pole k_n one may then write

$$G^+(x,x';k)=\frac{C_n(x,x')}{k-k_n}+\chi(x,x';k), \qquad \text{(A7)}$$

where $C_n(x,x';k)$ is the residue and $\chi(x,x';k)$ is regular at the pole. Substitution of Eq. (A7) into Eq. (A4) leads, after some simple algebra, to the result

$$\frac{1}{k-k_n}\left\{\frac{d^2C_n(x,x')}{dx^2}+[k^2-V(x)]C_n(x,x')\right\} +\left\{\frac{\partial^2\chi(x,x';k)}{\partial x^2}+[k^2-V(x)]\chi(x,x';k)\right\}-\delta(x-x') =0. \qquad \text{(A8)}$$

Taking the limit $k\to k_n$, the addition and substraction of $k_n^2C_n(x,x')/(k-k_n)$ to Eq. (A8) leads to the expressions

$$\frac{\partial^2C_n(x,x')}{\partial x^2}+[k_n^2-V(x)]C_n(x,x')=0 \qquad \text{(A9)}$$

and

$$\frac{\partial^2\chi(x,x';k_n)}{\partial x^2}+[k_n^2-V(x)]\chi(x,x';k_n)+2k_nC_n(x,x') =\delta(x-x'). \qquad \text{(A10)}$$

Now, substitution of Eq. (A7) into the boundary conditions given by Eqs. (A5) and (A6), adding and substracting $ik_nC_n(x,x')/(k-k_n)$, and taking the limit $k\to k_n$ yields

$$\left[\frac{\partial}{\partial x}C_n(x,x')\right]_{x=0_-}=-ik_nC_n(0,x'), \qquad \text{(A11)}$$

$$\left[\frac{\partial}{\partial x}\chi(x,x';k_n)\right]_{x=0_-}=-ik_n\chi(0,x';k_n)-iC_n(0,x'), \qquad \text{(A12)}$$

$$\left[\frac{\partial}{\partial x}C_n(x,x')\right]_{x=L_-}=ik_nC_n(L,x'), \qquad \text{(A13)}$$

and

$$\left[\frac{\partial}{\partial x}\chi(x,x';k_n)\right]_{x=L_-}=ik_n\chi(L,x';k_n)+iC_n(L,x'). \tag{A14}$$

One sees that Eq. (A9) for $C_n(x,x')$ and its boundary conditions (A11) and (A13) are identical to Eq. (A1) for $u_n(x)$ and its boundary conditions, (A2) and (A3). Consequently, these functions are proportional, namely,

$$C_n(x,x')=u_n(x)P(x'). \tag{A15}$$

An explicit expression for $P(x')$ may be obtained as follows. Multiply Eq. (A10) by $u_n(x)$ and Eq. (A1) by $\chi(x,x';k_n)$, subtract one from the other, and integrate from $x=0$ to $x=L$. The result may be written as

$$\left[u_n(x)\frac{\partial}{\partial x}\chi(x,x';k_n)-\chi(x,x';k_n)\frac{d}{dx}u_n(x)\right]_0^L+2k_n\int_0^L u_n(x)C_n(x,x')dx=\int_0^L u_n(x)\,\delta(x-x')dx. \tag{A16}$$

It then follows, using Eqs. (A2), (A3), (A12), (A14), and (A15), that

$$P(x')=\frac{u_n(x')}{2k_n\left\{\int_0^L u_n^2(x)dx+i[u_n^2(0)+u_n^2(L)]/2k_n\right\}}. \tag{A17}$$

Hence the residue of the outgoing Green's function at the pole k_n may be written as

$$C_n(x,x')=\frac{u_n(x)u_n(x')}{2k_n}, \tag{A18}$$

provided the resonant states are normalized according to the condition

$$\int_0^L u_n^2(x)dx+i\frac{u_n^2(0)+u_n^2(L)}{2k_n}=1. \tag{A19}$$

APPENDIX B: ASYMPTOTIC PROPERTIES OF THE MOSHINSKY FUNCTION

The Moshinsky function is defined as [18,11]

$$M(y)\equiv M(x,q,t)=\frac{i}{2\pi}\int_{-\infty}^{\infty}\frac{e^{ipx}e^{-ip^2t/\alpha}}{p-q}\,dp$$

$$=\frac{1}{2}e^{imx^2/2\hbar t}e^{y^2}\mathrm{erfc}(y), \tag{B1}$$

where the argument y is complex and q stands for $k, k_r\equiv a_r-ib_r$, or $k_{-r}=-k_r^*$. In this appendix we shall be interested in evaluating the limits as $t\to 0$ and as $t\to\infty$ of the Moshinsky function.

The properties of the M function may be obtained from the properties of the function $\exp(y^2)\mathrm{erfc}(y)$. It turns out that this last product corresponds to the function $w(z)=\exp(-z^2)\mathrm{erfc}(-iz)$ as defined by Abramowitz and Stegun [28] and Faddeyeva and Terent'ev [29]. Hence, making $z=iy$ one may write the M function as

$$M(y)=\frac{1}{2}e^{imx^2/2\hbar t}w(iy). \tag{B2}$$

Expression (B2) may be adequate for calculations since methods to evaluate numerically the function w are available [28,29]. The properties of the function w have been discussed by Abramowitz and Stegun [28] and Faddeyeva and Terent'ev [29].

For small values of the argument y it is convenient to consider the series expansion [28,29]

$$M(y)=\frac{1}{2}w(iy)=\frac{1}{2}\sum_{n=0}^{\infty}\frac{(-y)^n}{\Gamma(n/2+1)}. \tag{B3}$$

Hence, for $|y|\ll 1$,

$$M(y)\approx\frac{1}{2}\left[1-\frac{1}{2}\pi^{1/2}y+\cdots\right]. \tag{B4}$$

For very large values of the argument y, provided it obeys $-\pi/2<\arg y<\pi/2$, one may write the series expansion

$$w(iy)\approx\frac{1}{\pi^{1/2}y}-\frac{1}{\pi^{1/2}y^3}+\cdots, \tag{B5}$$

and therefore, using Eq. (B2), one may write $M(y)$ as

$$M(y)\approx\frac{1}{2}e^{imx^2/2\hbar t}\left[\frac{1}{\pi^{1/2}y}-\frac{1}{\pi^{1/2}y^3}+\cdots\right]. \tag{B6}$$

When the argument y lies within the limits $\pi/2<\arg y<3\pi/2$ one may use the symmetry relation

$$w(-iy)=2e^{y^2}-w(iy) \tag{B7}$$

to write the asymptotic expansion

$$w(-iy)\approx 2e^{y^2}-\frac{1}{\pi^{1/2}y}+\frac{1}{\pi^{1/2}y^3}-\cdots, \tag{B8}$$

and consequently, using Eq. (B2), one may write $M(y)$ as

$$M(y)\approx\frac{1}{2}e^{imx^2/2\hbar t}\left[2e^{y^2}-\frac{1}{\pi^{1/2}y}+\frac{1}{\pi^{1/2}y^3}+\cdots\right]. \tag{B9}$$

[1] A. P. Jauho and M. M. Nieto, Superlatt. Microstruc. **2**, 401 (1986).
[2] S. Collins, D. Lowe, and J. R. Barker, J. Phys. C **20**, 6233 (1987).
[3] T. B. Bhader, C. A. Morrison, and J. D. Bruno, Appl. Phys. Lett. **51**, 1089 (1987).
[4] H. Guo, K. Diff, G. Neofotistos, and J. D. Gunton, Appl. Phys. Lett. **53**, 131 (1988).
[5] J. A. Stovneng and H. A. Hauge, Phys. Rev. B **44**, 13 582 (1991).
[6] J. N. Muga and H. Cruz, Physica B **179**, 326 (1992).
[7] R. Tsu and L. Esaki, Appl. Phys. Lett. **22**, 452 (1973).
[8] E. E. Mendez, in *Physics and Applications of Quantun Wells and Superlattices*, edited by E. E. Mendez and K. Von Klitzing (Plenum, New York, 1987), p. 159.
[9] T. L. C. G. Sollner, E. R. Brown, W. D. Goddhue, and H. Q. Le, in *Physics of Quantum Electron Devices*, edited by F. Capasso (Springer-Verlag, Berlin, 1990) p. 147.
[10] G. García-Calderón (unpublished).
[11] M. Moshinsky, Phys. Rev. **88**, 625 (1952).
[12] W. Eberfeld and M. Kleber, Am. J. Phys. **56**, 154 (1988).
[13] M. Kleber, Phys. Rep. **236**, 331 (1994).
[14] See Sec. 11.6.3 in Peter R. Holland, *The Quantum Theory of Motion* (Cambridge University Press, Cambridge, 1993), and references therein.
[15] P. Szriftgiser, D. Guéry-Odelin. M. Arndt, and J. Dalibard, Phys. Rev. Lett. **77**, 4 (1996).
[16] See, for example, R. More, Phys. Rev. A **4**, 1782 (1973); G. García-Calderón, Lett. Nuovo Cimento **33**, 253 (1982), and references therein.
[17] G. García-Calderón, Solid State Commun. **62**, 441 (1987).
[18] M. Moshinsky, Phys. Rev. **84**, 525 (1951).
[19] H. M. Nussenzveig, in *Symmetries in Physics*, edited by A. Frank and K. B. Wolf (Springer-Verlag, New York, 1992) p. 293.
[20] G. García-Calderón, J. L. Mateos, and M. Moshinsky, Phys. Rev. Lett. **74**, 337 (1995).
[21] G. C. Hegerfeldt, Phys. Rev. Lett. **72**, 596 (1994).
[22] G. García-Calderón, R. Romo, and A. Rubio, Phys. Rev. B **47**, 9572 (1993).
[23] G. García-Calderón, A. Rubio, and J. Villavicencio (unpublished).
[24] L. Eisenbud, Ph.D. thesis, Princeton University, 1948 (unpublished), p. 88.
[25] D. Bohm, *Quantum Theory* (Prentice-Hall, New York, 1951), p. 291.
[26] See, for example, G. García-Calderón and A. Rubio, Solid State Commun. **71**, 237 (1989), and references therein.
[27] G. García-Calderón and R. E. Peierls, Nucl. Phys. A **265**, 443 (1976). Unfortunately, the derivation of the residue at a pole of the Green's function has a few typographical errors, though a careful reader may solve them without difficulty.
[28] *Handbook of Mathematical Functions*, edited by M. Abramowitz and I. A. Stegun (Dover, New York, 1965), p. 297.
[29] V. N. Faddeyeva and N. M. Terent'ev, *Mathematical Tables* (Pergamon, London, 1961).